A strategy to optimize precompression pressure for tablet manufacturing based on in-die elastic recovery

Gerrit Vreeman and Changquan Calvin Sun*

Pharmaceutical Materials Science and Engineering Laboratory, Department of Pharmaceutics, College of Pharmacy, University of Minnesota, Minneapolis, MN 55455, USA

*Corresponding Author

Changquan Calvin Sun, Ph.D.

9-127B Weaver-Densford Hall

308 Harvard Street S.E.

Minneapolis, MN 55455

Email: sunx0053@umn.edu

Tel: 612-624-3722

Abstract

A precompression pressure optimization strategy using in-die elastic recovery was developed to effectively address tablet lamination caused by air entrapment. This strategy involves exacerbating the air entrapment issue using high tableting speeds and main compaction pressures and collecting in-die elastic recovery data as a function of precompression pressure. The optimized precompression pressure, which corresponds to the minimum elastic recovery, is most effective at eliminating air from the powder bed prior to the main compression. When the optimized precompression pressure was employed, intact tablets of a model blend prone to lamination via air entrapment could be produced over a wide range of high main compaction pressures, while tablets without precompression laminated immediately after ejection at equivalent main compaction pressures. This optimization strategy is effective for addressing lamination issues due to air entrapment using precompression. An advantage of this strategy is that intact tablets are not required to identify an optimized precompression pressure since elastic recovery measurements occur in-die.

Keywords: lamination; precompression; air entrapment; tableting; elastic recovery

1 Introduction

Tablet lamination upon decompression or ejection is a common problem during pharmaceutical tablet manufacturing. Distinct from capping (Mazel and Tchoreloff, 2022), lamination is when a tablet splits into multiple layers along the tablet band (Alderborn and Frenning, 2018; Lee, 2010). The occurrence of lamination during formulation or process scale-up serves as an indication to modify key processing parameters or, in more severe cases, consider reformulation. Various approaches have been proposed to assess the tendency of powders to contain compression-induced defects (Akseli et al., 2013, 2014; Mazel et al., 2015b; Meynard et al., 2022; Paul and Sun, 2017) and identify their corresponding mechanism (Sinka et al., 2004; Wu et al., 2008, 2005). Identifying an effective solution to address lamination issues requires understanding their root causes. At least three lamination types have been identified, including air entrapment (Type 1), shear stress development during ejection (Type 2), and the development of tensile stresses in the tablet center for biconvex tablets (Type 3) (Long and Alderton, 1960; Mazel et al., 2018; Mazel and Tchoreloff, 2022). For Type 1 lamination, deaeration of the powder bed using a variety of techniques prior to a main compression event can be an effective solution since it minimizes the internal stress caused by the decompression of trapped air within the compact (Hiestand et al., 1977; Kalies et al., 2020; Tanino et al., 1995).

Type 1 lamination can be exacerbated by several factors (Long and Alderton, 1960), including 1) low powder bulk density or high initial air content, 2) high powder plasticity, which results in easier air entrapment by more readily sealing pores, 3) low clearance between the punch and die, which makes it more difficult for air to escape during compression (Mann et al., 1981), and 4) punches with a significant cup volume, which can force air from the cup into the compact during compression (Natoli et al., 2009). To alleviate Type 1 lamination, strategies such as

decreasing compression speed or increasing dwell time may be employed to allow more time for air to escape (Hiestand et al., 1977; Mazel and Tchoreloff, 2022; Tye et al., 2005). However, these strategies are less preferable due to the reduction in overall manufacturing throughput. Modifying the formulation composition or employing an optimized granulation process can also address air entrapment problems. However, these are not practical solutions for overcoming tablet lamination problems during the late stages of tablet development when the composition is locked. In contrast, powder deaeration using precompression is a highly convenient and commonly employed technique for mitigating Type 1 lamination issues (Mazel et al., 2015a; Mazel and Tchoreloff, 2022; Vezin et al., 1983; Vreeman and Sun, 2022a). This method is particularly advantageous as it does not reduce throughput and is readily accessible on most pharmaceutical rotary presses used for industrial tablet manufacturing (Sinka et al., 2009).

To identify the type of lamination, an assessment of the defect initiation (Garner et al., 2014; Yost et al., 2019), die wall pressure (Hiestand et al., 1977; Sugimori et al., 1989), tablet failure mode (Mazel et al., 2015a), the influence of processing parameters, and the effectiveness of lamination solution may be needed (Mazel and Tchoreloff, 2022). While visual observations of cracks in the tablet band may identify the presence and type of lamination, internalized lamination-like defects are more difficult to detect during development. These internal defects can unknowingly compromise tablet strength, artificially inflate measured tablet porosity, and increase the risk of failure during later processing phases, which is invariably more challenging to address (Sultan et al., 2023; Vreeman and Sun, 2022a). Detecting internal tablet cracks has typically required specialized methods such as X-ray microtomography (Schomberg et al., 2021; Wu et al., 2008). We have shown that, when Type 1 lamination is identified, in-die elastic recovery can be used as an effective parameter for diagnosing air entrapment and guiding strategies to mitigate

Type 1 lamination (Vreeman and Sun, 2022a). In this work, we develop and implement a strategy for optimizing precompression pressure to eliminate Type 1 tablet lamination by leveraging in-die elastic recovery measurements.

2 Materials and methods

2.1 Materials

Microcrystalline cellulose (MCC; Avicel® PH102, International Flavors & Fragrances, Philadelphia, PA) and magnesium stearate (MgSt; non-bovine, HyQual™, Mallinckrodt, St. Louis, MO) were used as received.

2.2 Mixing

MCC was blended with 2 % (w/w) MgSt in a blender (Turbula, Glen Mills, Clifton, NJ) for 5 min at 49 rpm. The total batch size was 100 g. At sufficiently high tableting speeds, this blend has been shown to reliably exhibit Type 1 lamination (Mazel and Tchoreloff, 2022).

2.3 Tableting

Tablets were prepared using a compaction simulator (Styl'One Evolution; MedelPharm, Beynost, France) simulating a Korsch XL100 (TSM B) press. The tableting speed was set to 60 rpm (34 ms dwell time, maximum upper punch velocity of 143 mm/s during precompression and 102 mm/s during the main compression) for default conditions and 120 rpm (17 ms dwell time, maximum upper punch velocity of 292 mm/s during precompression, 168 mm/s during the main compression) for fast conditions. Round, flat-faced punches and a straight bore die with an 11.28 mm diameter were used to compress 400 mg tablets (n = 3 per testing condition). Tablet weight was controlled by the die filling height, set at 10 mm. Precompression was employed at

various pressures ranging from 10 MPa to 150 MPa. Main compaction pressures of 150 MPa, 350 MPa, and 500 MPa were used.

2.4 Tablet tensile strength

Tablet dimensions (diameter, D, and thickness, t) were measured using a digital caliper (model CD-6"AX, Mitutoyo, Kawasaki, Kanagawa, Japan), and tablet breaking force (F) was measured using a texture analyzer (TA-XT2i; Texture Technologies Corporation, Scarsdale, NY). Tablet tensile strength (σ) was calculated using Equation 1 (Fell and Newton, 1970).

$$\sigma = \frac{2F}{\pi D t} \tag{1}$$

2.5 Tablet elastic recovery

Tablet in-die elastic recovery (ER) was calculated using Equation 2, where h_1 is the in-die thickness after decompression when the pressure approaches zero, and h_0 is the minimum thickness achieved during compression.

$$ER(\%) = \frac{h_1 - h_0}{h_0} * 100\% \tag{2}$$

The parameters h_0 and h_1 were extracted from the compaction simulator after correcting for machine deformation using an automated process in the Analis™ software. The upper and lower punches were pressed together in direct contact in an empty die up to a set force. Punch displacement as a function of force was measured and data was fitted with a second-degree polynomial equation to quantify the machine deformation, which was used to correct for the measured distance between punch tips when under load.

2.6 Tablet porosity

Tablet porosity (ε) was calculated using Equation 3, where ρ_{tablet} is the tablet density, calculated from measured tablet thickness, diameter, and weight, and ρ_t is the true density of the powder, which was taken as 1.4723 g/cm^3 (Vreeman and Sun, 2021). As MgSt was only present in low levels (2 %), its contribution to powder true density was considered negligible.

$$\varepsilon = 1 - \frac{\rho_{tablet}}{\rho_t} \quad (3)$$

3 Results and discussion

3.1 Effects of pressure and speed on tablet quality

Defect-free tablets of the model blend (Figure 1a) were produced using precompression pressures between 10 MPa and 100 MPa at a main compaction pressure of 150 MPa. When the main compaction pressure was increased to 350 MPa, defect-free tablets could only be made using precompression pressures between 30 MPa and 100 MPa. At a precompression pressure outside that range, either cracking in the tablet band (Figure 1b) or complete lamination of tablets (Figure 1c) was visually observed. At the main compaction pressure of 500 MPa, the range of precompression pressure for making defect-free tablets was further narrowed to between 40 MPa and 90 MPa. The simulation speed was increased from 60 rpm to 120 rpm at a main compaction pressure of 500 MPa to provide a worst-case scenario for air entrapment. This increase resulted in the narrowest range of precompression pressure, 60 MPa to 80 MPa, available for making intact tablets.

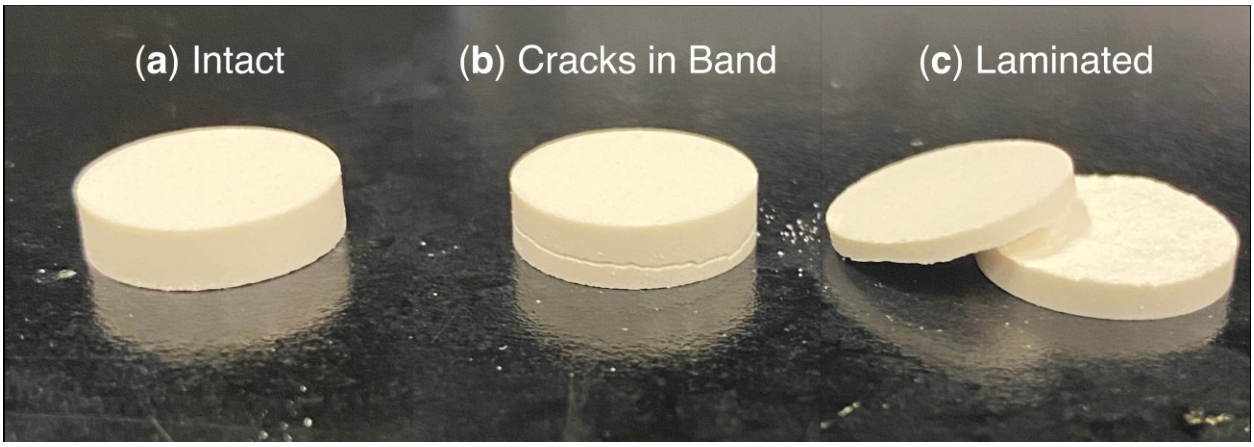

Figure 1. (a) An intact tablet, (b) a tablet exhibiting severe cracks in the tablet band, and (c) a laminated tablet.

From the qualitative visual observation of the tablet, defects caused by air entrapment are exacerbated by increasing the main compaction pressure. This finding aligns with a previous study that demonstrated a proportional increase in the detrimental effects on tablet mechanical properties with increasing compaction pressure (Vreeman and Sun, 2022a). In other words, a higher compaction pressure results in a more pronounced negative impact on the tablet's mechanical properties due to a higher internal pressure of entrapped air, which may be compounded by the higher elastic strain experienced by solid particles. Apart from the main compaction pressure, a faster compaction speed (120 rpm versus 60 rpm) exacerbated the occurrence of tablet defects (Figure 2). Consequently, the precompression pressure range within which defect-free tablets could be produced became narrower (Figure 2). This outcome may be rationalized based on the reduced time available for air to escape the compact as a result of the faster compression speed, leading to more trapped air and increased tablet defects. A faster speed can also result in less plastic deformation for viscoelastic materials, such as starch, due to the shorter compression duration (Tye et al., 2005). However, this mechanism is unlikely the main factor here since the compression properties of MCC are not sensitive to a change in speed (Tye et al., 2005).

The presence of a lower bound of precompression pressure for making intact tablets at each main compaction pressure reflects that a certain amount of time and powder consolidation is required to sufficiently deaerate the powder. The establishment of an upper precompression pressure limit for each main compaction pressure is justified because an excessive precompression pressure can lead to the entrapment of air within the compact of a highly plastic powder, which undergoes extensive plastic deformation and seals pores, preventing the escape of air during precompression (Mazel and Tchoreloff, 2022). Once the air is sealed in a tablet after precompression, a second main compression simply recompresses the already trapped air, resulting in lamination upon decompression. This observation aligns with previous studies that demonstrate the occurrence of capping at higher precompression pressures (Mazel and Tchoreloff, 2022, 2020). The upper bound precompression pressure is lower for more plastic materials because a lower pressure is required to induce plastic deformation.

From these observations, an optimal precompression pressure operating range for this blend is 60 MPa to 80 MPa, based on the worse-case scenario (i.e., operating at the highest pressure and speed). Choosing the pressure in the middle of this range (70 MPa, in this case) is preferred to ensure the production of intact tablets regardless of whether positive or negative deviation from the set precompression pressure is encountered. The main tableting pressure of 500 MPa exceeds typical pressures used for commercial tableting, and 120 rpm is the fastest operating speed for the simulated press in this work. However, if the tableting speed or main compaction pressure were increased further, convergence of the precompression pressure range for intact tablets to around 70 MPa would be expected. This example showcases a pitfall of setting the precompression pressure at a fixed percentage of the main compaction pressure, as tablets produced at 500 MPa

and 120 rpm with a 10% (50 MPa) precompression pressure would still exhibit borderline failure (Figure 2).

3.2 Tablet elastic recovery

In-die elastic recovery was previously used to demonstrate the presence of air entrapment in celecoxib tablets (Vreeman and Sun, 2022a). For this model blend, which exhibits Type 1 lamination (i.e., air entrapment) (Mazel and Tchoreloff, 2022), elastic recovery as a function of precompression pressure appears quadratic for all main compaction conditions (Figure 2).

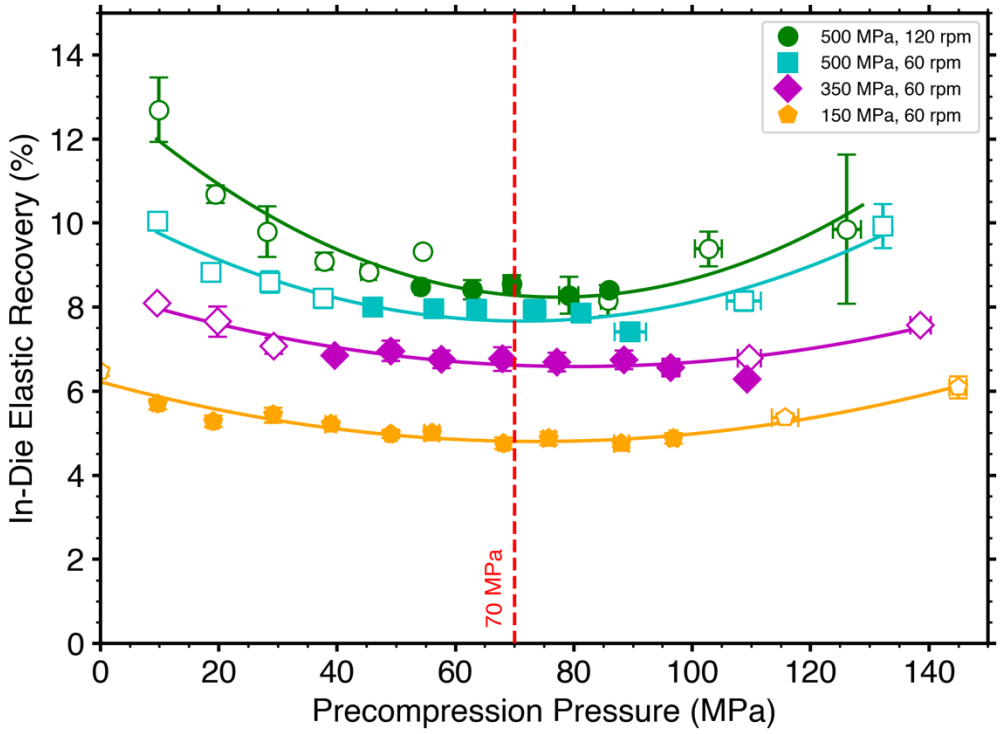

Figure 2. In-die tablet elastic recovery as a function of precompression pressure using different main compaction conditions. The dashed line at 70 MPa represents the identified optimized precompression pressure. Open symbols indicate tablets with visible lamination or cracking in the

band. Error bars showing standard deviation are present in the x and y directions, but some are hidden by the symbols (n = 3).

The measured in-die elastic recovery is a composite of solid particle elastic recovery and expansion of entrapped air. Since solid particle elastic recovery is essentially constant at a given main compaction condition regardless of precompression pressure, a lower elastic recovery corresponds to less entrapped air. Therefore, the minimum elastic recovery at a precompression pressure of 70 MPa indicates the condition with the least amount of entrapped air.

This quadratic trend can be explained by the interplay between powder consolidation and the kinetics of air escaping under different precompression pressures. Precompression both reduces the porosity of the powder bed and shrinks pores on the tablet surface due to more extensive particle plastic deformation. At the end of the precompression event, this initial powder bed densification reduces the volume available for air to occupy and increases the internal pressure of entrapped air. At a higher precompression pressure, the entrapped air is more compressed, which promotes air escape out of available pores before the main compaction event. At the same time, the smaller pore opening, or even sealed pores, hinders air escape. The interplay between the two opposite effects ultimately translates to the quadratic trend in in-die elastic recovery as a function of precompression pressure, with a minimum at ~70 MPa for this model blend (Figure 2).

The increase in overall elastic recovery as the main compaction pressure increases may be attributed to a larger extent of both solid particle elastic recovery and entrapped air volume expansion. At a main compaction pressure of 150 MPa (Figure 2, pentagons), the curvature of this trend is lower compared to that at higher main compaction pressures, showing a lower sensitivity of elastic recovery to a change in the precompression pressure. Although varying the precompression pressure resulted in different amounts of entrapped air in the tablets, the absolute

196 volume expansion of entrapped air during decompression was lower at this main pressure. Thus,
197 the contribution of air expansion to the overall tablet elastic recovery during decompression is
198 small compared to the elastic recovery of solid particles but is significant enough to cause
199 lamination when no precompression is used. However, at main compaction pressures of 350 MPa
200 and 500 MPa, the impact of air expansion on elastic recovery becomes more pronounced.
201 Therefore, the curvature of the elastic recovery versus precompression pressure curves increases,
202 corresponding to the more significant contribution of air expansion. In fact, at higher main
203 compaction pressures, the greater degree of air volume expansion during decompression caused
204 tablet defects over wider pressure ranges. This curvature was also amplified when the tablet
205 compression speed was increased from 60 rpm to 120 rpm at a compaction pressure of 500 MPa.
206 This observation is consistent with the expected larger amount of entrapped air within the tablet
207 due to the shorter amount of time available for the air to escape during the compression process.

208 Regardless of the degree of curvature, the minima of the parabola for each curve at all main
209 compaction conditions lies between 60 MPa and 80 MPa. Thus, the optimal precompression
210 pressure can be identified from an in-die elastic recovery profile at all speeds and main compaction
211 pressures investigated. However, a high main compression pressure and a high speed should be
212 used for locating the optimal precompression pressure due to the higher sensitivity.

213 **3.3 Tablet tensile strength**

214 Sufficient tablet strength is required for tablets to withstand the coating, packing, and
215 shipping conditions they may experience throughout their lifetime. Hence, the optimization of
216 precompression and main compression forces have traditionally relied on tablet performance
217 metrics, such as mechanical strength and friability, which are material-dependent (Gamlen et al.,
218 2015; Masilungan and Kraus, 1989; Ruegger and Çelik, 2000; Vezin et al., 1983). For example,

219 tablet tensile strength as a function of precompression pressure data can be used to identify
220 acceptable precompression pressures for making sufficiently strong tablets (Figure 3). Hence, we
221 compared the elastic recovery approach to the tablet performance-based traditional approach to
222 assess its potential as a surrogate method for precompression pressure optimization.

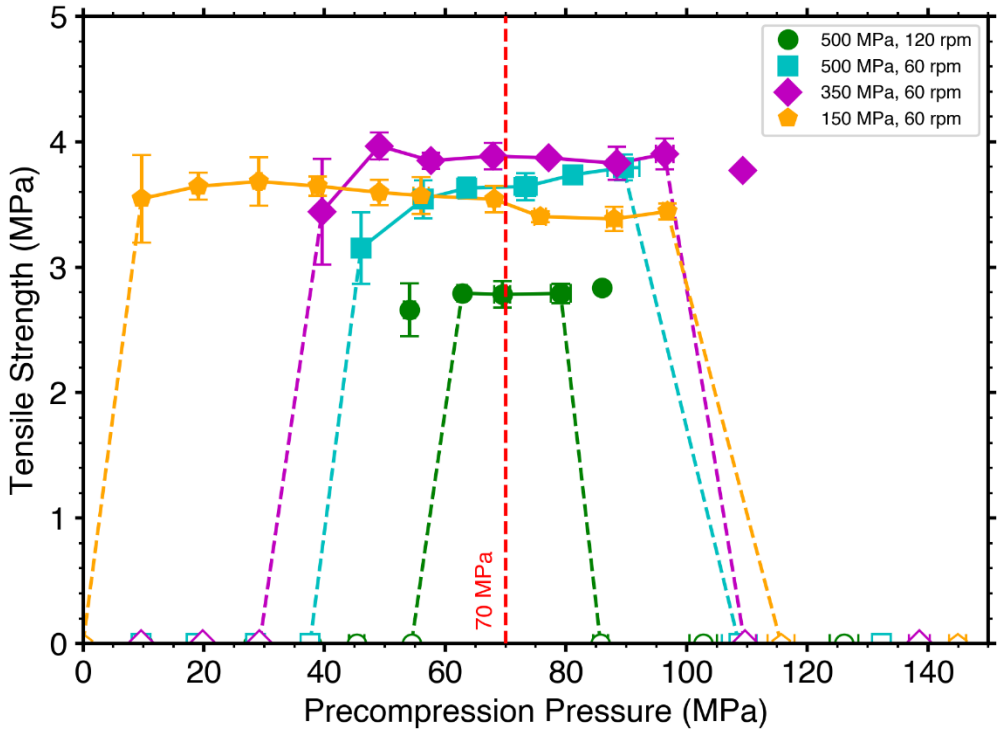

223

224 **Figure 3.** Tablet tensile strength as a function of precompression pressure using different main
225 compaction conditions. The dashed line at 70 MPa represents the identified optimized
226 precompression pressure. Open symbols indicate tablets with visible tablet defects, and
227 disconnected points represent borderline precompression pressures where both lamination and
228 intact tablets were obtained. Error bars showing standard deviation are present in the x and y
229 directions, but some are hidden by the symbols (n = 3).

230 Unlike the quadratic elastic recovery profiles (Figure 2), the relationship between tensile
231 strength and precompression pressure at a given main compaction pressure is a plateau (Figure 3).

In constructing Figure 3, visually defective tablets were assigned a tensile strength of 0 MPa. Borderline precompression pressures, where both visually intact tablets and laminated tablets were observed, occurred at ~110 MPa at a main compaction pressure of 350 MPa at 60 rpm and precompression pressures of ~50 MPa and ~90 MPa at a main compaction pressure of 500 MPa and a speed of 120 rpm. At the lowest precompression pressure at which visibly intact tablets could be made, diametrical tablet breaking was observed (10 MPa for a main compaction pressure of 150 MPa at 60 rpm, 40 MPa for a main compaction pressure of 350 MPa at 60 rpm, 45 MPa for a main compaction pressure of 500 MPa at 60 rpm, and 55 MPa for a main compaction pressure of 500 MPa at 120 rpm). However, the standard deviation of tensile strength is relatively high, likely indicating the presence of internalized defects or cracks within the compact as a result of incomplete deaeration, weakening the compact and decreasing the tensile strength. Thus, this precompression pressure should also be avoided to ensure optimum tablet mechanical properties.

Tensile strength does not significantly change between main compression pressures of 150 MPa, 350 MPa, and 500 MPa at 60 rpm, indicating that tensile strength as a function of main compression pressure nears a plateau in the pressure range of 150 MPa to 500 MPa at this compaction speed. A lower tablet tensile strength was observed when the compression speed was increased to 120 rpm. This reduction may be due to a higher elastic recovery by more entrapped air (Figure 2), a lower extent of particle plastic deformation due to faster compression speeds, or both. The precompression pressure at the middle of the tensile strength plateau roughly agrees with the minimum identified from the elastic recovery plot (Figure 2). However, tensile strength requires multiple out-of-die tablet parameters, including tablet diameter, thickness, and breaking force, which are not required for the in-die elastic recovery assessment. Therefore, the in-die elastic

recovery assessment appears to be more efficient than the traditional tensile strength-based assessment for identifying an optimum precompression pressure to avoid Type 1 tablet lamination.

3.4 Effects of optimized precompression pressure on tabletability

The tabletability (tablet tensile strength versus main compaction pressure) of the MCC mixed with 2 % MgSt blend was evaluated with and without an optimized precompression (Figure 4). When no precompression was used (Figure 4, circles), intact tablets may be formed up to about 100 MPa, but any further increase causes tablet lamination. When a precompression pressure of 70 MPa was employed (Figure 4, squares), a typical tabletability profile approaching a plateau tensile strength of 4.2 MPa was observed (Figure 4) (Vreeman and Sun, 2022b).

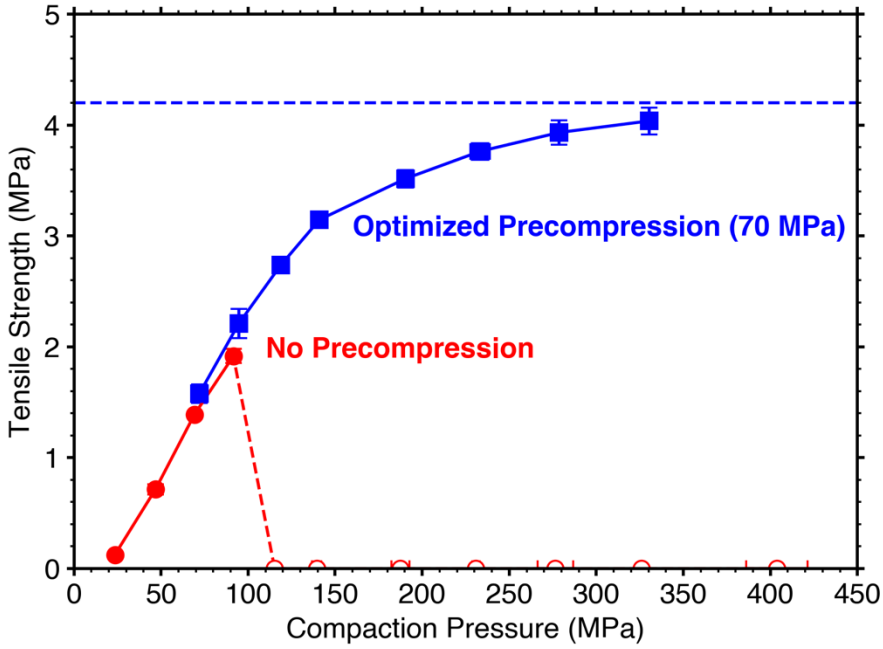

Figure 4. Tabletability of MCC mixed with 2 % MgSt with (squares) and without (circles) a 70 MPa precompression pressure. Tablet lamination is indicated by open shapes at a tensile strength of zero. Main compaction pressures below 70 MPa are not included in the precompression-optimized curve because the optimized precompression pressure would be greater

than the main compression pressure. Error bars showing standard deviation are present in the x and y directions, but some are hidden by the symbols (n = 3).

At compaction pressures where the two tabletability profiles overlap (75 MPa and 100 MPa), tablets prepared with a precompression pressure of 70 MPa exhibited slightly higher tensile strength. This difference may be attributed to two possible reasons: 1) The longer total compression time accounting for both precompression and main compression steps since strain rate sensitivity of this blend was observed (Figure 3); 2) More residual air in compacts produced without precompression at this borderline pressure reduced the bonding area due to more extensive air expansion after decompression. Tablets may be further weakened if excessive elastic recovery due to air expansion leads to internal defects.

To experimentally explore this, we investigated the differences in bonding area and bonding strength by analyzing their compressibility and compactibility profiles (Sun, 2011). The compressibility profiles are essentially superimposed (Figure 5b). Hence, the use of precompression pressure of 70 MPa did not cause detectable porosity differences despite the reduced elastic recovery (Figure 5a) when precompression was employed, indicating similar bonding areas. An analysis of compactibility (Figure 5c) using the Ryshkewitch-Duckworth model (Duckworth, 1953; Ryshkewitch, 1953) shows no statistically significant (p = 0.05) difference in apparent bonding strength, as measured by σ_0 (6.50±2.17 MPa with no precompression, 4.94±0.13 MPa with a 70 MPa optimized precompression). However, it is difficult to quantitatively compare compactibility at these conditions since low porosity tablets cannot be produced without precompression and high porosity tablets cannot be produced when employing a 70 MPa optimized precompression step. When the two sets of data are combined, the σ_0 (5.1±0.22 MPa) is not significantly different from that for the data with precompression

(4.94±0.13 MPa). These results suggest that the impact of precompression pressure on bonding area and bonding strength of this blend cannot be captured by compressibility and compactibility analyses due to the subtleness of the structural change. In reality, the difference in tensile strength at these overlapping pressures could be a combination of both material viscoelasticity and different amounts of entrapped air.

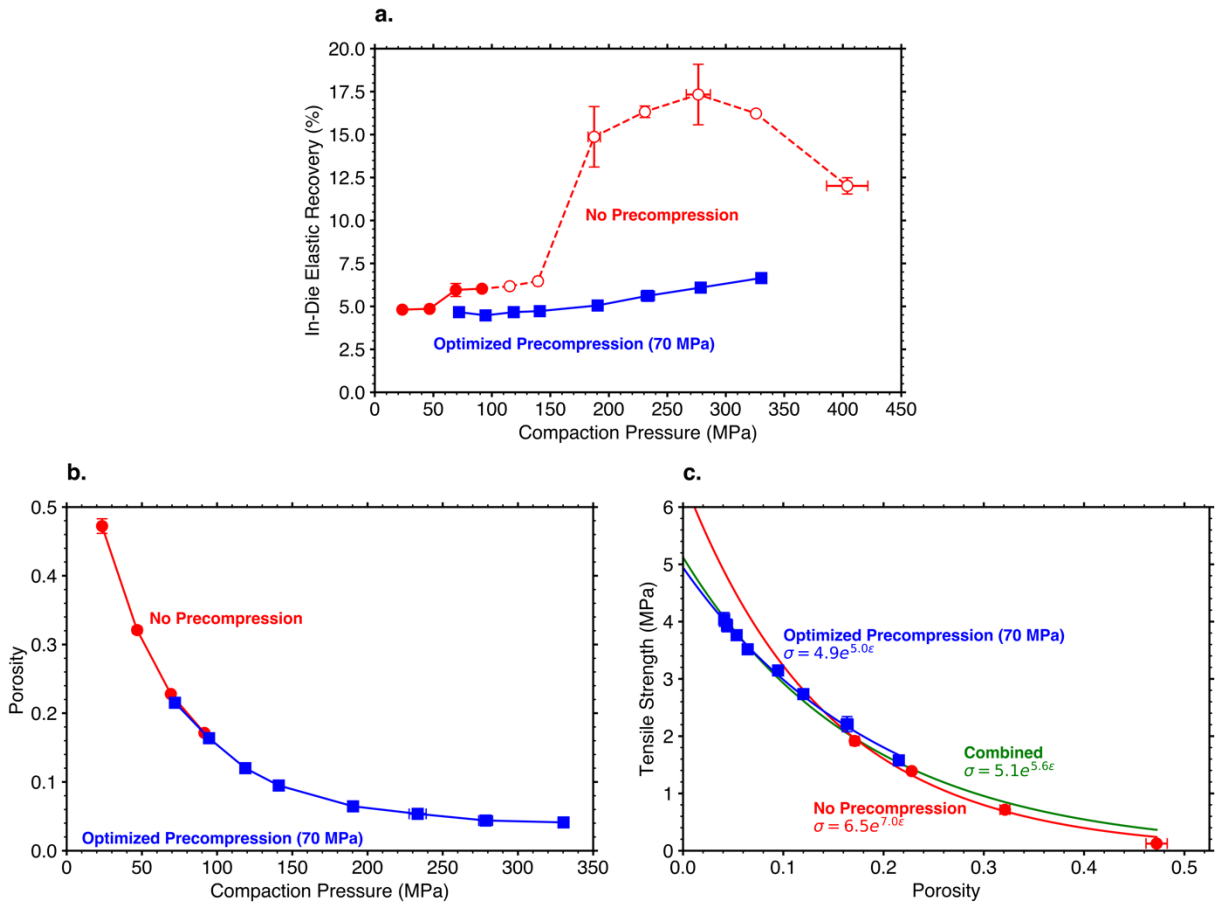

Figure 5. (a) Elastic recovery versus compaction pressure, (b) compressibility, and (c) compactibility of MCC mixed with 2 % MgSt with (squares) and without (circles) optimizing precompression pressure. Error bars showing standard deviation are present in the x and y directions, but some are hidden by the symbols (n = 3). Open circles signify tablets with visible lamination.

Interestingly, the elastic recovery profile of the blend without precompression (Figure 5a, circles) shows a small (1 %) increase in elastic recovery when the main pressure increased from 50 MPa to 70 MPa, and a large (8 %) increase in elastic recovery from 150 MPa to 190 MPa. This small initial increase may indicate the onset of air entrapment at ~70 MPa, which is close to the optimal precompression pressure identified in Figure 2. The subsequent large increase may be attributed to the extensive volume expansion of entrapped air during the decompression phase. This profile is similar to a previous study, which reported a large increase in elastic recovery due to air entrapment (Vreeman and Sun, 2022a). When the optimized precompression pressure of 70 MPa was applied (Figure 5a, squares), the elastic recovery profile was smooth and continuous, suggesting the effectiveness of the precompression step in minimizing air entrapment.

3.5 A strategy for precompression optimization

Based on these results, we propose the following two-step process for optimizing the precompression pressure to mitigate or even eliminate Type 1 lamination during powder compression:

1. Collect the in-die elastic recovery as a function of precompression pressure at the highest operating speed and main compaction pressure available.
2. The precompression pressure corresponding to the minimum in-die elastic recovery is determined and taken as the optimal precompression pressure.

If elastic recovery is not sensitive to variations in precompression pressure under the conditions in step 1, there is no need to employ precompression as Type 1 lamination is either unlikely to be a problem for those materials, or precompression will not be an effective solution. If lamination and tablet defects are still observed when the optimal precompression pressure is employed, other strategies, such as using a tapered die, increasing punch-die clearance,

changing the cup concavity of the punches, or reducing compression speed, should be explored to alleviate defects (Mazel and Tchoreloff, 2022). Additionally, Type 2 or Type 3 lamination may play a role and could be further investigated. If in-die elastic recovery is unavailable, other tablet properties, such as tensile strength or friability as a function of precompression pressure, can be characterized to identify the acceptable operating precompression pressures. If a range of acceptable precompression pressures is identified, the midpoint of the range should be targeted to allow for maximum process variability while still achieving an acceptable product for enhanced robustness of the tablet manufacturing process.

4 Conclusion

We have demonstrated an efficient strategy to optimize precompression pressure using in-die elastic recovery as a function of precompression pressure at a given main compaction pressure and tableting speed. These in-die elastic recovery profiles follow a quadratic trend, and the minimum corresponds to the precompression pressure that should be targeted to remain in the middle of the optimal range of this process parameter. This systematic process for determining an optimal precompression pressure for a given powder can be adopted to guide efficient tablet formulation design in a material-sparing manner. In-die elastic recovery assessment allows for an understanding of the air entrapment tendency of powders during powder compression. Its simplicity, sensitivity, and ease of implementation and interpretation indicate its possible utility as an in-process parameter, along with other parameters, such as ejection force and peak compression pressure, for monitoring the tablet manufacturing process and ensuring batch-to-batch consistency of tablet quality. Accordingly, rotary tablet presses with the ability to measure in-die elastic recovery may hold an advantage over traditional press designs in terms of in-line process control. Further studies at borderline conditions where only internal defects occur may help further

demonstrate potential benefits of this approach in guiding tablet formulation optimization. In addition, validating this strategy with a realistic, multicomponent tablet formulation prone to Type 1 lamination may help facilitate the adoption of this method in pharmaceutical industry.

Acknowledgements

Funding from the National Science Foundation through grant number IIP- 1919037, AFPE through 2022 Dr. Paul B. Myrdal Memorial Pre-Doctoral Fellowship, and Department of Pharmaceutics, UMN, through David and Marilyn Grant Fellowship in Physical Pharmacy (2022-2023) is gratefully acknowledged for partially supporting GV. CCS thanks the National Science Foundation for support through the Industry University Collaborative Research Center grant IIP-2137264, Center for Integrated Materials Science and Engineering for Pharmaceutical Products (CIMSEPP).

References

Akseli, I., Ladyzhynsky, N., Katz, J., He, X., 2013. Development of predictive tools to assess capping tendency of tablet formulations. Powder Technol. 236, 139–148. https://doi.org/10.1016/j.powtec.2012.04.026

Akseli, I., Stecu\la, A., He, X., Ladyzhynsky, N., 2014. Quantitative correlation of the effect of process conditions on the capping tendencies of tablet formulations. J. Pharm. Sci. 103, 1652–1663. https://doi.org/10.1002/jps.23951

Alderborn, G., Frenning, G., 2018. Tablets and compaction, in: Aulton's Pharmaceutics: The Design and Manufacture of Medicines. Elsevier, pp. 517--563.

Duckworth, W., 1953. Discussion of Ryshkewitch paper by Winston Duckworth. J. Am. Ceram. 36, 68–68. https://doi.org/10.1111/j.1151-2916.1953.tb12838.x

Fell, J.T., Newton, J.M., 1970. Determination of tablet strength by the diametral-compression test. J. Pharm. Sci. 59, 688–691. https://doi.org/10.1002/jps.2600590523

Gamlen, M.J.D., Martini, L.G., Al Obaidy, K.G., 2015. Effect of repeated compaction of tablets on tablet properties and work of compaction using an instrumented laboratory tablet press. Drug Dev. Ind. Pharm. 41, 163–169. https://doi.org/10.3109/03639045.2013.850715

Garner, S., Ruiz, E., Strong, J., Zavaliangos, A., 2014. Mechanisms of crack formation in die compacted powders during unloading and ejection: An experimental and modeling comparison between standard straight and tapered dies. Powder Technol. 264, 114–127. https://doi.org/10.1016/j.powtec.2014.04.086

Hiestand, E.N., Wells, J.E., Peot, C.B., Ochs, J.F., 1977. Physical processes of tableting. J. Pharm. Sci. 66, 510–519. https://doi.org/10.1002/jps.2600660413

Kalies, A., Heinrich, T., Leopold, C.S., 2020. A novel approach to avoid capping and/or lamination by application of external lower punch vibration. Int. J. Pharm. 580, 119195. https://doi.org/10.1016/j.ijpharm.2020.119195

Lee, B.-J., 2010. Pharmaceutical preformulation: Physicochemical properties of excipients and powders and tablet characterization, in: Pharmaceutical Sciences Encyclopedia. John Wiley & Sons, Ltd, pp. 1–54. https://doi.org/10.1002/9780470571224.pse362

Long, W.M., Alderton, J.R., 1960. The displacement of gas from powders during compaction. Powder Metall. 3, 52–72. https://doi.org/10.1179/pom.1960.3.6.004

Mann, S.C., Bowen, D.B., Hunter, B.M., Roberts, R.J., Rowe, R.C., Tracy, R.H.T., 1981. The influence of punch tolerance on capping. J. Pharm. Pharmacol. 33, 25P. https://doi.org/10.1111/j.2042-7158.1981.tb11684.x

Masilungan, F.C., Kraus, K.F., 1989. Determination of precompression and compression force levels to minimize tablet friability using simplex. Drug Dev. Ind. Pharm. 15, 1771–1778. https://doi.org/10.3109/03639048909052400

Mazel, V., Busignies, V., Diarra, H., Tchoreloff, P., 2015a. Lamination of pharmaceutical tablets due to air entrapment: Direct visualization and influence of the compact thickness. Int. J. Pharm. 478, 702–704. https://doi.org/10.1016/j.ijpharm.2014.12.023

Mazel, V., Diarra, H., Busignies, V., Tchoreloff, P., 2015b. Evolution of the die-wall pressure during the compression of biconvex tablets: Experimental results and comparison with FEM simulation. J. Pharm. Sci. 104, 4339–4344. https://doi.org/10.1002/jps.24682

Mazel, V., Diarra, H., Malvestio, J., Tchoreloff, P., 2018. Lamination of biconvex tablets: Numerical and experimental study. Int. J. Pharm. 542, 66–71. https://doi.org/10.1016/j.ijpharm.2018.03.012

Mazel, V., Tchoreloff, P., 2022. Lamination of pharmaceutical tablets: Classification and influence of process parameters. J. Pharm. Sci. 111, 1480–1485. https://doi.org/10.1016/j.xphs.2021.10.025

Mazel, V., Tchoreloff, P., 2020. Role of precompression in the mitigation of capping: A case study. J. Pharm. Sci. 109, 3210–3213. https://doi.org/10.1016/j.xphs.2020.07.021

Meynard, J., Amado-Becker, F., Tchoreloff, P., Mazel, V., 2022. On the complexity of predicting tablet capping. International Journal of Pharmaceutics 623, 121949. https://doi.org/10.1016/j.ijpharm.2022.121949

Natoli, D., Levin, M., Tsygan, L., Liu, L., 2009. Development, optimization, and scale-up of process parameters: Tablet compression, in: Qiu, Y., Chen, Y., Zhang, G.G.Z., Liu, L., Porter, W.R. (Eds.), Developing Solid Oral Dosage Forms. Academic Press, San Diego, pp. 725–759. https://doi.org/10.1016/B978-0-444-53242-8.00032-1

Paul, S., Sun, C.C., 2017. Gaining insight into tablet capping tendency from compaction simulation. Int. J. Pharm. 524, 111–120. https://doi.org/10.1016/j.ijpharm.2017.03.073

Ruegger, C.E., Çelik, M., 2000. The influence of varying precompaction and main compaction profile parameters on the mechanical strength of compacts. Pharm. Dev. Technol. 5, 495–505. https://doi.org/10.1081/PDT-100102033

Ryshkewitch, E., 1953. Compression strength of porous sintered alumina and zirconia. J. Am. Ceram. 36, 65–68. https://doi.org/10.1111/j.1151-2916.1953.tb12837.x

Schomberg, A.K., Diener, A., Wünsch, I., Finke, J.H., Kwade, A., 2021. The use of X-ray microtomography to investigate the microstructure of pharmaceutical tablets: Potentials and comparison to common physical methods. Int. J. Pharm. X 3, 100090. https://doi.org/10.1016/j.ijpx.2021.100090

Sinka, I.C., Cunningham, J.C., Zavaliangos, A., 2004. Analysis of tablet compaction. II. Finite element analysis of density distributions in convex tablets. J. Pharm. Sci. 93, 2040–2053. https://doi.org/10.1002/jps.20111

Sinka, I.C., Motazedian, F., Cocks, A.C.F., Pitt, K.G., 2009. The effect of processing parameters on pharmaceutical tablet properties. Powder Technol. 189, 276–284. https://doi.org/10.1016/j.powtec.2008.04.020

Sugimori, K., Mori, S., Kawashima, Y., 1989. Characterization of die wall pressure to predict capping of flat- or convex-faced drug tablets of various sizes. Powder Technol. 58, 259–264. https://doi.org/10.1016/0032-5910(89)80052-X

Sultan, T., Dave, V.S., Cetinkaya, C., 2023. Early detection and assessment of invisible cracks in compressed oral solid dosage forms. Int. J. Pharm. 635, 122786. https://doi.org/10.1016/j.ijpharm.2023.122786

Sun, C.C., 2011. Decoding powder tabletability: Roles of particle adhesion and plasticity. J. Adhes. Sci. Technol. 25, 483–499. https://doi.org/10.1163/016942410X525678

Tanino, T., Aoki, Y., Furuya, Y., Sato, K., Takeda, T., Mizuta, T., 1995. Occurrence of capping due to insufficient air escape during tablet compression and a method to prevent it. Chem. Pharm. Bull. 43, 1772–1779. https://doi.org/10.1248/cpb.43.1772

Tye, C.K., Sun, C.C., Amidon, G.E., 2005. Evaluation of the effects of tableting speed on the relationships between compaction pressure, tablet tensile strength, and tablet solid fraction. J. Pharm. Sci. 94, 465–472. https://doi.org/10.1002/jps.20262

Vezin, W.R., Pang, H.M., Khan, K.A., Malkowska, S., 1983. The effect of precompression in a rotary machine on tablet strength. Drug Dev. Ind. Pharm. 9, 1465–1474. https://doi.org/10.3109/03639048309052388

Vreeman, G., Sun, C.C., 2022a. Air entrapment during tablet compression – Diagnosis, impact on tableting performance, and mitigation strategies. Int. J. Pharm. 615, 121514. https://doi.org/10.1016/j.ijpharm.2022.121514

Vreeman, G., Sun, C.C., 2022b. A powder tabletability equation. Powder Technol. 408, 117709. https://doi.org/10.1016/j.powtec.2022.117709

Vreeman, G., Sun, C.C., 2021. Mean yield pressure from the in-die Heckel analysis is a reliable plasticity parameter. Int. J. Pharm. X 3, 100094. https://doi.org/10.1016/j.ijpx.2021.100094

Wu, C.-Y., Hancock, B.C., Mills, A., Bentham, A.C., Best, S.M., Elliott, J.A., 2008. Numerical and experimental investigation of capping mechanisms during pharmaceutical tablet compaction. Powder Technol. 181, 121–129. https://doi.org/10.1016/j.powtec.2006.12.017

Wu, C.-Y., Ruddy, O.M., Bentham, A.C., Hancock, B.C., Best, S.M., Elliott, J.A., 2005. Modelling the mechanical behaviour of pharmaceutical powders during compaction. Powder Technol. 152, 107–117. https://doi.org/10.1016/j.powtec.2005.01.010

Yost, E., Chalus, P., Zhang, S., Peter, S., Narang, A.S., 2019. Quantitative X-ray microcomputed tomography assessment of internal tablet defects. J. Pharm. Sci. 108, 1818–1830. https://doi.org/10.1016/j.xphs.2018.12.024